Power Management Architecture for Universal Input Ac-Dc Adapter Support in Battery Powered Applications

S. M. Ahsanuzzaman, Justin Blackman, Mor M. Peretz, and Aleksandar Prodić
Laboratory for Power Management and Integrated SMPS,
ECE Department, University of Toronto, CANADA
E-Mail: {ahsansm,prodic}@ele.utoronto.ca

Acknowledgements

Keywords

«DC power supply», «Switched-mode power supply», «Converter circuit», «High frequency power converter », «Power management»

Abstract

This paper introduces a novel power management architecture for battery powered portable applications, where ac-dc power adapters are used to charge the battery. The flyback-based system allows independent regulation of output bus voltage, irrespective of adapter output, and battery cell voltages. This architecture creates the flexibility to use a wide range of adapters to power the device while charging the battery cells. The effectiveness of the introduced architecture is verified on a 20-W, 100 kHz experimental prototype. Experimental results demonstrate tight output bus voltage regulation over a wide range of adapter-provided dc inputs and smooth transitions between adapter and battery powered modes of operation.

I. Introduction

Modern battery-powered portable electronic devices, such as cell phones, laptops, tablet PCs, portable DVD players, and the like, use ac-dc wall adapters to recharge their enclosed batteries. These electronic devices require a wide range of fixed input voltages for proper operation. Today, depending on the application, output voltages of power adapters range between 5 V and 20 V [1]. The wide variety of the device requirements creates a burden for the user who, alongside portable devices, needs to carry a number of device-specific power adapters, which are often bulky.

The requirement for the use of an application specific adapter is related to the power management system of a portable device, whose typical architecture is shown in Fig.1 [2]. The system consists of a battery charger, dc-dc bus voltage converter, and a set of point of load (PoL) dc-dc converters supplying functional blocks. Depending on the conversion ratio and power rating the PoL can be realized as switch mode power supply (SMPS) or low-dropout (LDO) linear regulators. A set of switches for reconfiguring the system depending on the mode of operation is also often included. Here, when the adapter is connected, switch SW_1 is turned on, switch SW_2
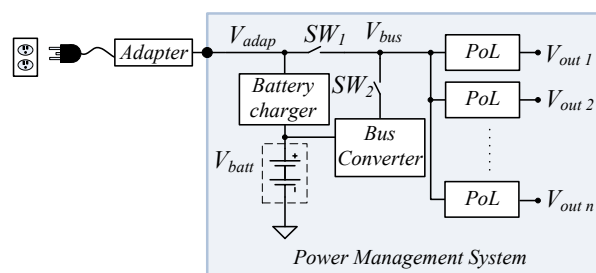

Fig.1: Conventional laptop power management system

is turned off and the adapter is used for both providing the bus voltage (V_{bus}) and battery charging [3]. When the adapter is unplugged, SW_1 is turned off, SW_2 is turned on and the battery provides the bus voltage, through the dc-dc bus converter. In both of these modes, i.e. adapter-powered and battery-powered, the bus voltage is the same. Other voltages, required by

Introduced Power Management System

Fig.2: Universal-input power management system

various functional blocks of the device, are derived from the bus voltage, using downstream dc-dc SMPS and linear LDOs.
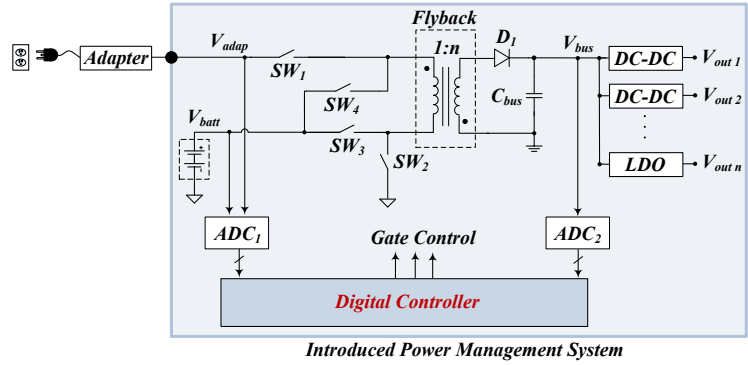
The presented conventional architecture has a significant drawback of imposing a fairly strict limit on the adapter output voltage. This limit comes from the fact that the bus and the adapter voltages need to be approximately the same, since the efficiency and dynamic performance of the downstream stages are strongly affected by the bus voltage variations [4]. The adapter voltage is further constrained by the limitations imposed by the internal battery charging converter and its required input voltages. As a consequence, dedicated device-based adapters are usually needed for laptop and tablet computers, mobile phones and all other devices we use.

The goal of this paper is to introduce a simple universal-input power management system architecture that eliminates the need for application-specific adapters by allowing a wide range of dc input voltages to be connected to a battery-powered portable device. The new flyback-converter based architecture, shown in Fig.2, breaks the fairly strict three-way dependence between the bus (V_{bus}), battery (V_{batt}), and adapter (V_{adap}) voltages existing in the conventional solutions. Also, the new architecture is well suited for incorporating emerging programmable bus voltage techniques, where the bus voltage is dynamically varied to optimize the overall system efficiency [5]. Furthermore, the power management architecture eliminates the need for application-specific battery packs, potentially allowing a wider range of battery packs to be used with a given portable device.

II. System Description and Principle of Operation

The core element of the power management system architecture of Fig.2 is a flyback-based converter. The following subsections explain its operation in three distinct modes of operation: i) adapter-powered bus regulation and battery charging, ii) adapter-powered bus regulation only, which is utilized when the battery is fully charged, and iii) battery-powered bus regulation.

A. Adapter-powered bus regulation and battery charging

In this mode of operation, both the bus voltage regulation and battery charging are provided. The sequence of gating signals for proper converter operation is selected based on the adapter and battery voltages. The following subsections discuss the introduced converter operation for both higher and lower adapter voltages compared to the battery voltage.

1) Operation for $V_{adap} \geq V_{batt}$

Fig.3a shows the circuit configuration and the key converter waveforms for the case when the adapter voltage is higher than the battery voltage. Those include the gating signals of all three switches, the magnetizing inductance current and the battery charging current.

In this mode SW_4 is not used, hence it is always off, and the switching period T_{sw} has three distinctive intervals. The switch SW_1 is turned on during the first two intervals, providing the input current from the adapter. During the first interval, labeled as d_1T_{sw}, the magnetizing inductance is charged and, during the second and third intervals, the stored energy is distributed between the battery and the bus, respectively. This is achieved by operating SW_2 with a duty ratio d_1 and by gating SW_3 with duty ratio d_2 to charge the battery. In the third interval, when SW_1 is turned off, the magnetizing inductor current flows through the transformer, and hence transfers the energy to the bus through the diode D_1. As shown in Fig.3a, when SW_2 is on, the magnetizing inductor current has a slope of V_{adap}/L_m,

Fig.3a: Adapter-powered mode of operation when $V_{adap} \geq V_{batt}$. Top: converter configuration; Bottom: key converter waveforms

where V_{adap} is the adapter output voltage and L_m is the magnetizing inductance. During the conduction of SW_3, the slope is changed to $(V_{adap}-V_{batt})/L_m$, where V_{batt} is the battery voltage. Since in this case V_{batt} is smaller than V_{adap}, a positive slope of magnetizing inductance current occurs when SW_3 conducts.

It can be found that the relation between the three voltages in this mode is described with the following equation:

$$V_{bus} = n \cdot V_{adap} \cdot \frac{d_1 + d_2}{1 - d_1 - d_2} - n \cdot V_{batt} \cdot \frac{d_2}{1 - d_1 - d_2} \tag{1}$$

where d_1 and d_2 are the duty ratio values of switches SW_2 and SW_3, respectively. This equation shows that, by adjusting d_1 and d_2, both the bus voltage regulation and the charging of the battery can be achieved independent of the adapter voltage value. It also shows that the rigid correlation between the battery, adapter, and bus voltages existing in the conventional architecture is eliminated. As described in section III, the digital controller of Fig.1 sets the two duty ratio values, such that the desired bus voltage regulation and battery charging profile are achieved. The controller also provides seamless mode transitions.
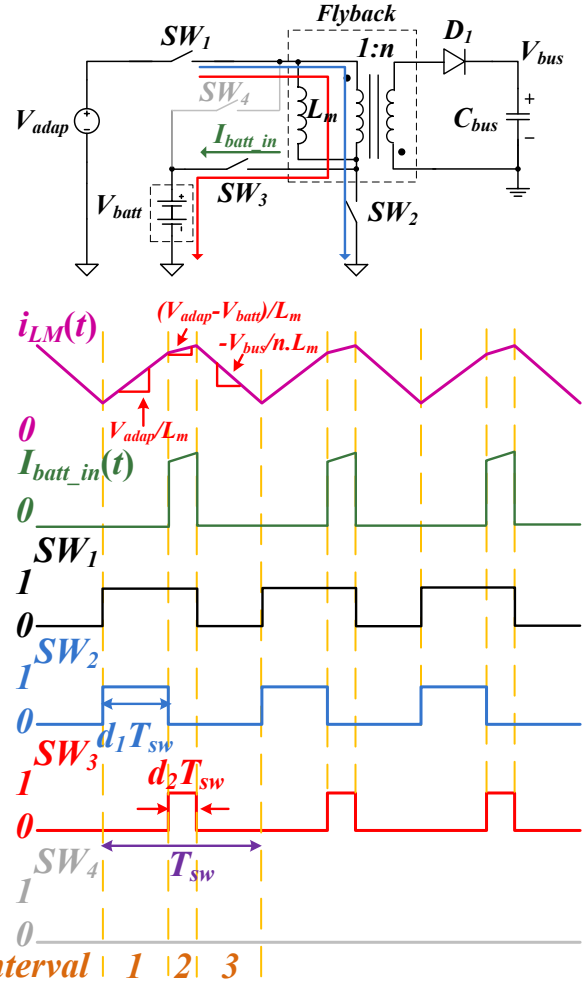
2) Operation for $V_{adap} < V_{batt}$

Fig.3b shows the circuit configuration and the key converter waveforms, for the case when the adapter voltage is lower than the battery voltage.

The gating sequence in this mode of operation is similar to those for $V_{adap} \geq V_{batt}$ situation. However, in this case, there is a major difference affecting the transformer design. When SW_3 is turned on, during the second interval, a negative voltage is applied across the magnetizing inductor (in Fig.3b indicated by, the negative slope of its current). This means that on the secondary side of the flyback transformer the reflected voltage is also opposite, possibly causing conduction of the diode, $D1$. To prevent this, the turns ratio of the flyback transformer n can be selected such that it satisfies the following equation:

$$n \cdot (V_{batt} - V_{adap}) < V_{bus} \qquad (2)$$

B. Adapter-powered bus regulation only

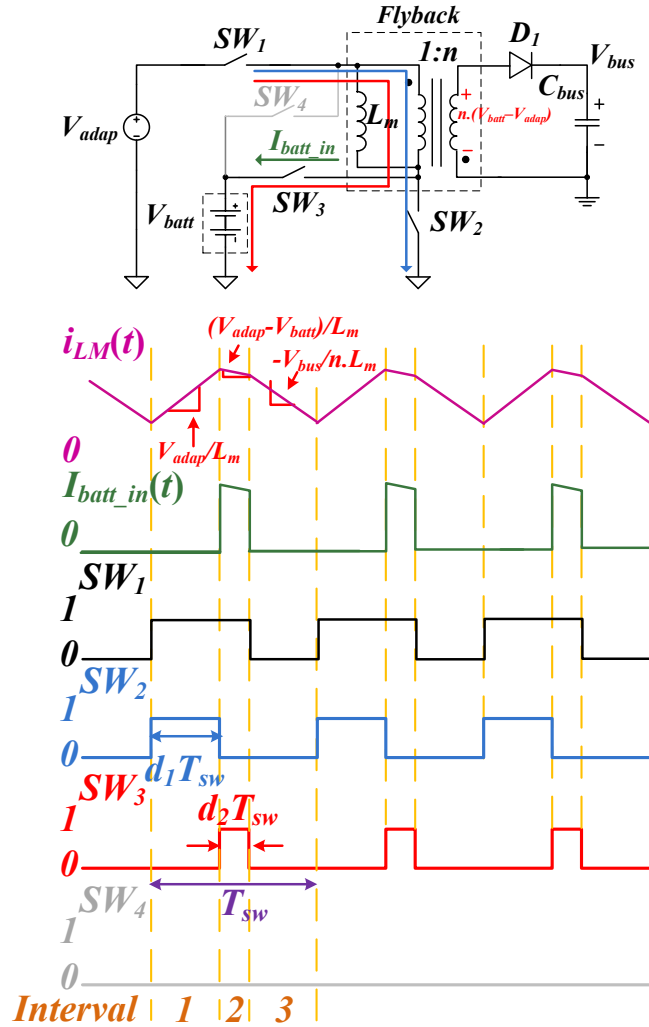The adapter-powered bus regulation only mode is activated when the battery is fully charged, and hence, there is no

Fig.3b: Adapter-powered mode of operation when $V_{adap} < V_{batt}$. Top: converter configuration; Bottom: key converter waveforms

need for further charging. In this mode, the converter operates as a conventional flyback. Here, the previously described interval 2 of Figs.3a and 3b is eliminated by turning off both SW_1 and SW_2 at the end of the first interval. Throughout this mode, SW_3 and SW_4 are kept off and the conversion ratio is:

$$V_{bus} = n \cdot V_{adap} \cdot \frac{d_1}{1 - d_1} \qquad (3)$$

where, d_1 is the duty ratio for SW_1 and SW_2. The adapter-to-bus steady-state conversion ratio for this mode can also be found from equation (1), by setting d_2 to zero.

C. Battery-powered bus regulation

Fig. 4 demonstrates the operation of the power management module when an adapter is not connected and the battery powers the device. In this case SW_1 and SW_3 are always turned off, SW_2 is kept on and SW_4 operates at a switching frequency $f_{sw} = 1/T_{sw}$, with duty ratio d. When SW_4 is turned on, V_{batt} is seen across the transformer primary side. When SW_4 is turned off, the diode D_1 conducts. This

operating mode is similar to that of the conventional flyback converter. Hence, the ideal battery-to-bus voltage conversion ratio is:

$$V_{bus} = n \cdot V_{batt} \cdot \frac{d}{1-d} \qquad (4)$$

The equation shows that the bus voltage can be regulated without imposing a strict limitation on the battery pack voltage. Therefore, a large flexibility in selecting battery packs for a given device is provided. It is important to note that the direction of the magnetizing inductor current is the same in all three modes of operation, allowing smooth mode transitions.

III. Practical Implementation

A practical implementation of the introduced power management system, including switch realization, is shown in Fig.5. The figure also shows a block diagram of the digital controller.

Fig.4: Battery-powered mode of operation Top: converter configuration; Bottom: key converter waveforms

A. Power stage

The four switches on the primary side of the flyback transformer in Fig.5 (labeled SW_{1-4}) enable the desired multi-mode operation. In this case the transistor SW_5 replaces diode D_1 of Fig.2, to minimize the conduction loss. SW_4 is realized with back-to-back transistors providing bi-directional voltage blocking and thus, allowing battery voltage V_{batt} to be higher or lower than V_{adap}. The back-to-back connection also prevents the magnetizing inductance current from flowing through SW_3 and SW_4 when SW_2 is turned off in adapter-powered mode of operation. Also, as mentioned earlier, during battery powered mode (Fig.4), SW_4 is turned off rather than SW_2, to prevent the primary side current circulating through SW_4 and the body diode of SW_3. An RCD snubber [6] is incorporated to provide over-voltage protection from the flyback-transformer's leakage inductance current.

B. Digital Controller

The multi-mode digital controller of Fig.5 regulates both the bus voltage and the battery charging process. The *Mode Control* module generates various gating sequences for SW_{1-5}, depending on the state-of-charge of the battery, and detects the presence of the adapter. The presence of adapter and battery voltage level are detected through *Mux* and the analog-to-
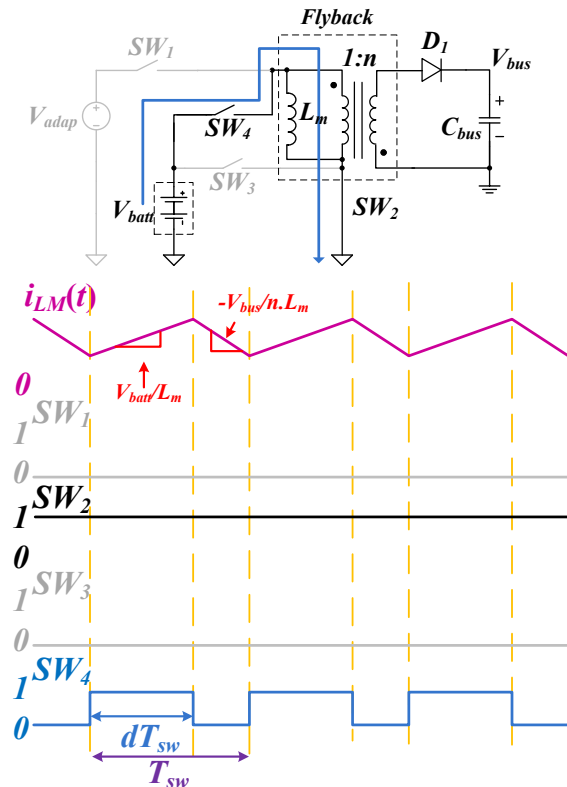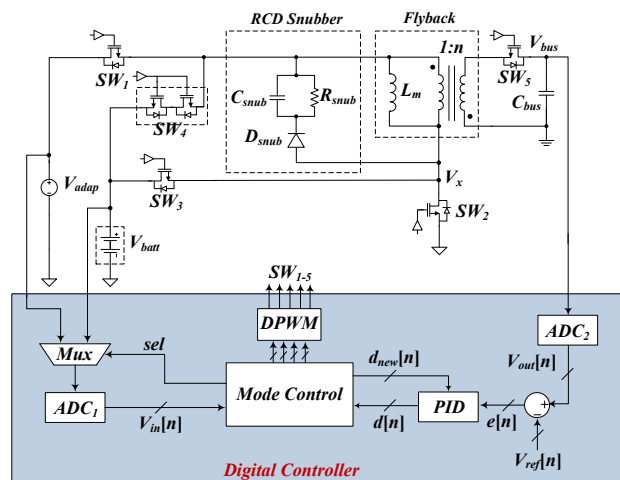
Fig.5: Practical implementation of the introduced architecture

digital converter ADC_1. This module periodically samples both V_{adap} and V_{batt} to detect the adapter input and to monitor the battery voltage, preventing overcharging of the battery.

1) Bus voltage regulation in Battery-powered or adapter-powered mode

When simultaneous battery charging and bus regulation is not required, the converter operates as a conventional digital voltage-mode pulse-width modulated system [7], [8]. An analog-to-digital converter, ADC_2 senses the bus voltage and, after a comparison with the desired reference $V_{ref}[n]$, an error signal $e[n]$ is created. This signal is fed to a PID compensator. The digital duty ratio command generated by the PID, $d[n]$, is then passed to a multi-input multi-output DPWM module through the *Mode Control* module, creating the signals as previously described in *Section II*.

2) Combined battery charging with bus voltage regulation, mode transitions and soft start

When the battery voltage drops, indicating that charging is needed, gating pulses are sent to SW_3 immediately after SW_2 turns off, providing pulsating currents to the battery cells, as described in *Section II*. This dual pulse injection can create a sub-transient response in the output voltage, requiring the PID to update the duty command for this new steady-state operation. In order to reduce the perturbation of the output voltage from the battery cell charging, the width of the SW_3 gate pulses is slowly incremented from zero. This soft-starting mechanism allows the controller to gradually adjust the duty ratio, providing a seamless transition.

A duty ratio predicting method is implemented in order to achieve a smooth transition after connection or disconnection of the adapter. In this method, a new initial duty command $d_{new}[n]$ is determined based on the new operating mode and the corresponding past and present input voltages. This duty information is then sent to the PID module to set up the initial duty ratio for the gating signals in the new operating mode.

IV. EXPERIMENTAL SYSTEM AND RESULTS

To verify the operation of the universal-input power management system, a 20 W, 100 kHz experimental prototype was developed. The results obtained with the experimental setup are shown in Figs. 6 to 13.

Fig.6: Steady-state operation in battery charging mode, when V_{adap}=9V,V_{batt}=3V,V_{bus}=5V

Fig.7: Magnified steady-state operation in battery charging mode, when V_{adap}=9V,V_{batt}=3V,V_{bus}=5V

Fig.6 shows the steady-state operation of the converter in the presence of a 9 V adapter and a 3 V battery, where both the bus voltage regulation at 5 V and battery charging are simultaneously performed. The results confirm that, for the newly introduced topology, a dedicated adapter with a voltage close to the bus value is not needed. It can be seen that the bus voltage is well regulated, even though relatively large differences between the adapter, bus, and battery voltage values exist. Fig.7 shows a magnified version of the steady state current waveforms with the slopes indicated.

Fig.8: Steady-state operation in battery charging mode, when V_{adap}=9V, V_{batt}=7.5V, V_{bus}=5V
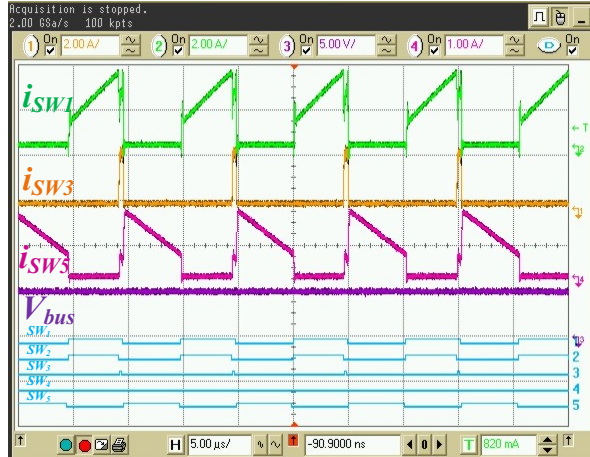

Fig.9: Magnified steady-state operation in battery charging mode, when V_{adap}=4V, V_{batt}=6V, V_{bus}=5V

Fig.8 shows simultaneous system operation of 5 V bus regulation and battery charging when adapter voltage is 9 V and battery voltage is 7.5 V. The result verifies that the introduced architecture is able to regulate the bus when both adapter and battery voltages are higher than the bus voltage. Fig.9 shows the waveforms for the case when the adapter voltage is lower (4V) and battery voltage is higher (6V) than the bus voltage (5V). This verifies the proper system operation for V_{adap}<V_{batt}.

Fig.10: Steady-state operation from battery input, when V_{batt}=7.5V, V_{bus}=5V
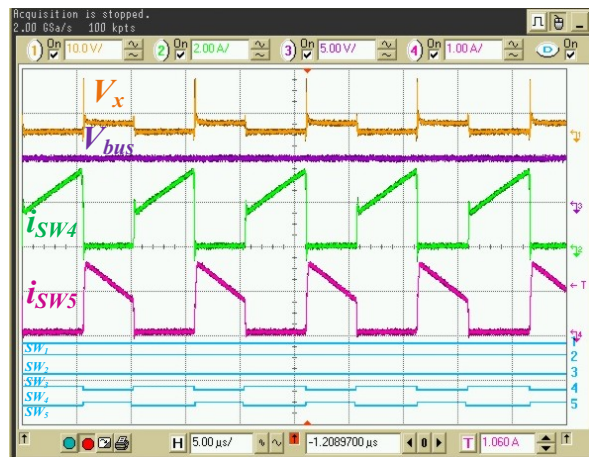

Fig.11: Steady-state operation from battery input, when V_{batt}=3V, V_{bus}=5V

Figs.10 and 11 show the system operation from the battery when the battery voltage is 7.5V and 3V, respectively. These waveforms demonstrate tight bus voltage regulation irrespective of the battery voltage.
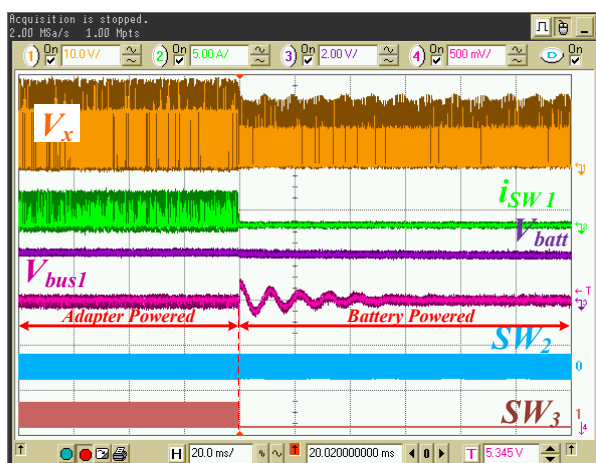
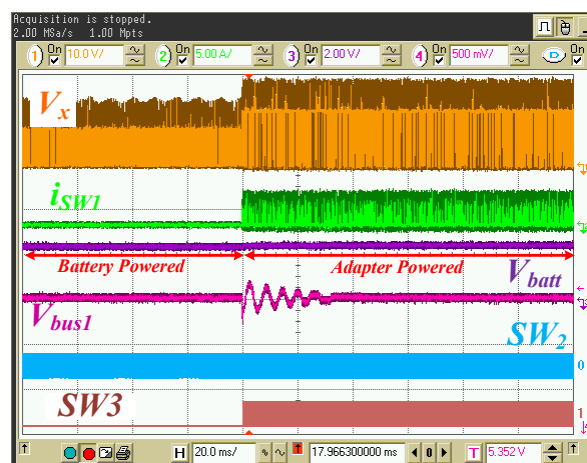Fig.12: Transition from adapter-powered mode to battery-powered mode

Fig.13: Transition from battery-powered mode to adapter-powered mode

Figs.12 and 13 show transitions between the adapter-powered and the battery-powered modes of operation during the adapter connections/disconnection process. Fairly smooth transitions causing no larger than 200 mV variation of the bus voltage are achieved, which is comparable to those of state of the art solutions [2].

V. CONCLUSIONS

A universal-input flyback-based power management architecture is introduced. It allows a wide range of dc voltages to be connected to the inputs of portable devices, eliminating the need for device-specific ac-dc adapters. The architecture also potentially allows a wider range of battery packs to be used with a given battery powered portable device. The new topology and its complementary digital controller allow smooth transitions between the adapter and battery supplied modes of operation. Experimental verification with a 20W prototype fully confirms functionality of the new universal-input power management system.

References

[1] Panepinto, P.A.; , "Making power adapters smarter and greener," *Sustainable Systems and Technology, 2009. ISSST '09. IEEE International Symposium on* , vol., no., pp.1-5, 18-20 May 2009.

[2] Harfman-Todorovic, M.; Palma, L.; Enjeti, P.; , "A Hybrid DC-DC Converter for Fuel Cells Powered Laptop Computers," Power Electronics Specialists Conference, 2006. PESC '06. 37th IEEE , vol., no., pp.1-5, 18-22 June 2006.

[3] Cleveland, T.L.; , "Bi-directional power system for laptop computers," Applied Power Electronics Conference and Exposition, 2005. APEC 2005. Twentieth Annual IEEE , vol.1, no., pp.199-203 Vol. 1, 6-10 March 2005

[4] Qahouq, J.A.A.; Muralidhar, G.; , "Control Scheme for High-Efficiency High-Performance Two-Stage Power Converters," Applied Power Electronics Conference and Exposition, 2009. APEC 2009. Twenty-Fourth Annual IEEE , vol., no., pp.1226-1232, 15-19 Feb. 2009

[5] Ahsanuzzaman, S.M.; McRae, T.; Mahdavikhah, B.; Prodic, A.; , "Programmable-output PFC rectifier with dynamic efficiency and transient response optimization," Applied Power Electronics Conference and Exposition (APEC), 2012 Twenty-Seventh Annual IEEE , vol., no., pp.285-290, 5-9 Feb. 2012

[6] Peipei Meng; Xinke Wu; Jianyou Yang; Henglin Chen; Zhaoming Qian; , "Analysis and design considerations for EMI and losses of RCD snubber in flyback converter," Applied Power Electronics Conference and Exposition (APEC), 2010 Twenty-Fifth Annual IEEE , vol., no., pp.642-647, 21-25 Feb. 2010

[7] Patella, B.J.; Prodic, A.; Zirger, A.; Maksimovic, D.; , "High-frequency digital controller IC for DC/DC converters," Applied Power Electronics Conference and Exposition, 2002. APEC 2002. Seventeenth Annual IEEE , vol.1, no., pp.374-380 vol.1, 2002

[8] Syed, A.; Ahmed, E.; Maksimovic, D.; Alarcon, E.; , "Digital pulse width modulator architectures," Power Electronics Specialists Conference, 2004. PESC 04. 2004 IEEE 35th Annual , vol.6, no., pp. 4689- 4695 Vol.6, 20-25 June 2004.